Acta Astronautica 238 (2026) 769–778

Contents lists available at ScienceDirect

Acta Astronautica

journal homepage: www.elsevier.com/locate/actaastro

Research paper

Constraining Earth's orbital capacity via operational feasibility☆

William E. Parker *,1, Maya Harris 1, Giovanni Lavezzi, Richard Linares

Department of Aeronautics and Astronautics, Massachusetts Institute of Technology, 77 Massachusetts Ave, Cambridge, 02139, MA, USA

ARTICLE INFO

Dataset link: https://celestrak.org, https://space-track.org

Keywords:
Capacity
Space sustainability
Conjunction assessment

ABSTRACT

Earth's orbital environment has grown increasingly congested as the cost of satellite deployment has fallen dramatically in the twenty-first century. In the absence of cost constraints, other limitations, including sustainability considerations, may soon become the primary barriers to further expansion. Assessments of orbital carrying capacity help map these emerging constraints to sustainable levels of satellite activity. While most prior efforts in defining capacity have focused on constraining satellite populations to avoid runaway debris growth, other factors also warrant attention. This work introduces an operational feasibility constraint that limits the acceptable rate of close approaches between tracked objects, beyond which the cadence of collision avoidance maneuvers would make operations infeasible. Using the full public U.S. catalog of two-line elements in low Earth orbit, approximate conjunction nodes are identified based on Keplerian orbit geometries. The resulting operational capacity framework is used to evaluate the sustainability of current orbital populations and to identify key trends in recent history to inform future deployments and operator behavior. By defining operational criticality, occupation, and capacity in consistent and interpretable units, this work shows how satellite populations interact and, if overpopulated or uncoordinated, stifle each other's ability to operate effectively.

1. Introduction

The concept of carrying capacity has been used for decades in conservation ecology to describe the maximum number of individuals an ecosystem can indefinitely sustain without degradation [1]. The carrying capacity of any system is determined by constraints, which vary depending on what exactly we seek to sustain. In recent years, space sustainability advocates have developed measures of satellite carrying capacity in Earth's orbit to establish thresholds on space activity that would prevent long-term degradation of the space environment. First, they must identify what a sustainable future in space looks like. For some, a sustainable future is achieved when all operators strictly follow existing policy guidelines [2]. For others, ideal development utilzes new coordination schemes like orbital slotting [3]. For most, it is a future that avoids the runaway debris growth and cascading collisions of Kessler Syndrome [4]. Once a sustainable future is defined, researchers must identify which factors contribute to that future and decide how those factors map to fundamental constraints. For avoiding Kessler Syndrome, the constraint is population stability, which is impacted by operational factors such as the rate of collisions or rate of debris population growth [5,6]. Ongoing work is also being done to develop risk indices, which combine several environmental factors together into one number [7,8]. Indices may further be used to identify derived constraints which are mapped from the fundamental constraints to units more interpretable for satellite operators and regulators.

Despite these significant efforts, a unified definition of orbital capacity and a consensus on how to measure current populations' occupation of that capacity remain elusive within the field. This lack of consensus stems, in part, from differing interpretations of what a sustainable future in space looks like. While there are many constraints that could feasibly be applied to orbital capacity, various stakeholders prioritize these constraints differently, leading to divergent assessments.

As mentioned previously, much of the existing work on orbital capacity focuses on the dynamical stability of the space environment [2, 9–13]. These frameworks aim to avoid a Kessler syndrome scenario by limiting satellite collisions, explosions, and launch rates. They evaluate the long term sustainability by evolving existing satellite and debris populations over decades or centuries to identify stable and unstable paths forward.

☆ A portion of this research has been previously presented at the 11th Annual Space Traffic Management Conference, Austin, Texas, March 4–5, 2025 under the title "Defining Orbital Capacity through Operational Feasibility".

* Corresponding author.
E-mail addresses: wparker@mit.edu (W.E. Parker), mharris4@mit.edu (M. Harris), glavezzi@mit.edu (G. Lavezzi), linaresr@mit.edu (R. Linares).

1 These authors contributed equally to this work.

https://doi.org/10.1016/j.actaastro.2025.09.055
Received 2 July 2025; Received in revised form 16 September 2025; Accepted 17 September 2025
Available online 24 September 2025

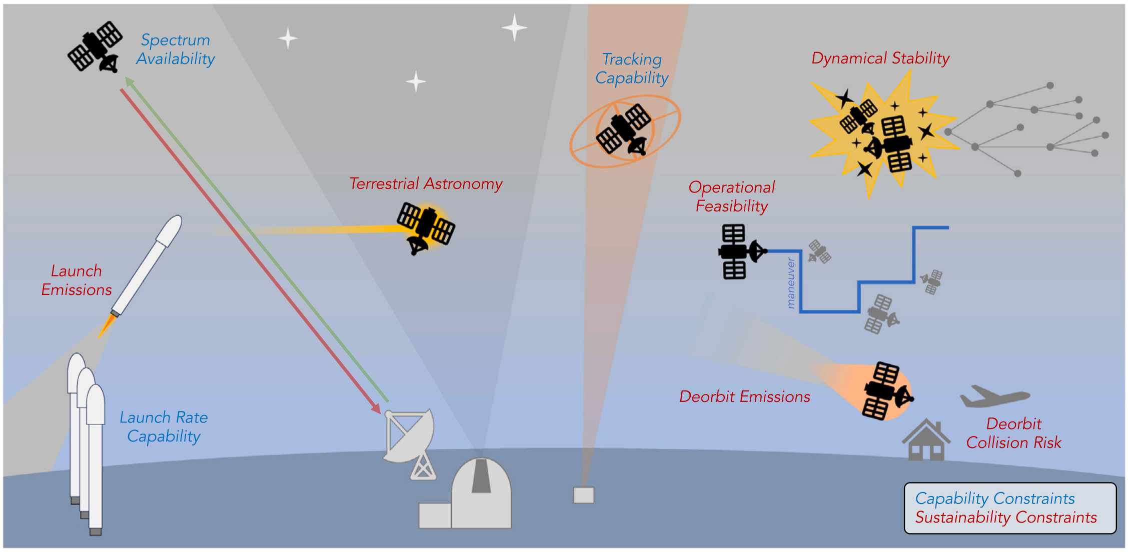

Fig. 1. Orbital capacity is constrained by capability limitations and sustainability issues.

These existing approaches consider orbital population properties like counts, object masses, object sizes, disposal mechanisms, or risk indices to assess the dynamical stability of orbital populations. However, there are many additional constraints beyond dynamical stability worth considering, some of which are shown in Fig. 1. *Capability constraints* on launch cadence [14], spectrum sustainability [15], and satellite tracking [16] impose fundamental limits on the number of satellites that may be effectively operated based on technological capability or physical limitations. Technological advances help to increase the limits set by these constraints. In contrast, *sustainability constraints* are determined by the environment and enable continued viable satellite operations in the future. Some examples of sustainability constraints include dynamical stability, radio and optical interference for terrestrial astronomy [17], ground safety risk [18], and atmospheric pollution during satellite launch [19] and reentry [20].

Ultimately, the appropriate choice of constraints depends on the specific objective. If the primary goal is to prevent a cascading debris scenario, then dynamical stability should be prioritized. This work, however, emphasizes sustained operational feasibility. For satellite operations to remain viable, the rate of close approaches—or conjunctions—between spacecraft must be kept low. If collision risk becomes too high or operators are forced to constantly perform avoidance maneuvers, continued operations may no longer be practical. This feasibility constraint is distinct from the requirement to avoid debris cascades. At low altitudes where atmospheric drag is large, exceeding a dynamical stability threshold is unlikely, but operational feasibility may still be compromised if satellite populations are too large. Because different constraints dominate in different orbital regions, the overall capacity is set by the most restrictive constraint in each region.

Many previous orbital sustainability assessments do not account for the impact of structure and coordination on capacity. Structured satellite deployments—common in large constellations—along with enhanced space domain awareness and advanced collision avoidance technologies, can enable safer operation in densely occupied regions, provided the supporting infrastructure is highly robust [3]. Disordered, uncoordinated satellite trajectories lead to regular conjunctions that require burdensome mitigation action [10]. Realistic orbital populations are partially ordered (i.e. well-managed, coordinated constellations), and partially disordered (i.e. debris populations and uncoordinated individual satellites from small operators). Since space traffic coordination is one of the lowest cost options for reducing collision risk between satellites, capacity frameworks should be able to account for structure as a variable subject to change.

To the authors' knowledge, this work is the first to explicitly incorporate satellite conjunction rates as a constraint on the sustainable scale and distribution of satellite operations in Earth's orbit. This new constraint complements existing dynamical stability-defined capacity metrics, as it seeks to prevent a separate undesirable outcome in low Earth orbit (LEO) that is related to but distinct from the problem of long-term runaway debris growth. The sustainability assessments in this work are produced from snapshots of the orbital population from two-line elements (TLEs) in the public U.S. satellite catalog to best represent realistic structure in orbital populations. The results of this operational feasibility study present capacity, occupation, and criticality as distinct quantities with consistent units, enabling straightforward attribution of environmental impact to individual satellites while also highlighting the broader system-level constraints on satellite populations. Keplerian dynamics are presumed based on the mean orbit elements from the TLE sets to produce a fast approximate analytical assessment of short-term conjunction risk and operational feasibility.

The paper is organized as follows: Section 2 reviews and proposes clarified definitions for orbital capacity, criticality, and occupation. Section 3 outlines the methodology for fast analytical conjunction node assessment that is used for assessing operational feasibility. Section 4 presents the results from an analysis of the existing population of tracked objects in LEO. Concluding remarks are provided in Section 5.

2. Distinguishing capacity, criticality, and occupation

Today, satellite operators are encouraged to follow sustainable best practices to minimize their impact on the orbital environment [21–23]. These practices include ensuring that satellites are trackable and maneuverable, share data, and deorbit soon after mission completion. Even if all satellites followed these guidelines, their combined presence would still degrade the environment. While a bottom-up approach, where sustainability is promoted by reducing the environmental impact of each individual satellite, helps mitigate harm, it does not map to the population-level capability or sustainability constraints. Sustainability in orbit requires coordination and a consideration of system-wide limitations, not just responsible individual behavior. A truly sustainable framework should evaluate satellite impact in aggregate based on population-level environmental constraints on capacity, ensuring that each satellite's environmental impact contribution is assessed in the context of the broader system.

Part of the challenge in the field of space sustainability is the lack of clear and consistent vocabulary. While the terms *capacity* and *criticality* appear frequently in the literature, they are used inconsistently and sometimes interchangeably. Part of the confusion stems from the fact that capacity is sometimes defined as the aggregation of criticality over a certain population [24]. In practice, it is common to calculate the aggregate value of a risk or criticality metric for a population that appears sustainable, and to then adopt that value as a proxy for capacity [8]. This approach sidesteps the more fundamental task: selecting the actual threshold that defines the environmental constraint we care about.

In this work, we posit that *capacity* should refer to constraint-driven limits on sustainable space activity that quantify the amount of orbital resource that is available. In contrast, we consider *criticality* a measure of a spacecraft's (or a population's) impact on the space environment. Most space sustainability metrics that have been developed so far are criticality metrics; they often combine different properties of a spacecraft (i.e. mass, cross-sectional area, orbit parameters, etc.) and produce a metric that is proportional to the amount of risk the spacecraft presents to the surrounding environment [7,25,26]. While these metrics are very useful for comparing the *relative* impact of different satellites on their environment, they do not correlate directly to capacity, which is defined by population-level constraints.

The term *occupation* is rarely used in assessments of orbital sustainability but is essential for distinguishing between key variables in the broader space sustainability framework. Occupation serves as the complement to capacity, representing how much of the available orbital resource is currently being utilized. While capacity is influenced by environmental variability, such as long-term climate change in the thermosphere [12], occupation can be actively managed through sustainable best practices by satellite operators. In other words, while the total available orbital resource is largely fixed, its efficient use can be optimized through coordination and sustainability measures that minimize unnecessary occupation. For example, satellite collision avoidance does not increase capacity but does reduce occupation for a set number of satellites. For these distinctions to be meaningful, capacity should not be measured simply as the number of satellites but rather in terms that reflect the system's fundamental constraints.

To ensure clear interpretation of individual impacts on the overall system, capacity, criticality, and occupation should be measured in consistent units. Establishing interpretable, standardized metrics and thresholds is crucial for enabling regulators, operators, and the public to accurately assess risks, understand the severity of orbital congestion problems, and implement effective strategies for sustainable space operations. This work proposes definitions for capacity, criticality, and occupation that are constrained by operational feasibility and defined in units of number of conjunctions per month.

3. The operationally feasible capacity

3.1. Conjunction screening and nodes

We consider a *conjunction* to be a close approach between two objects that likely requires risk-mitigation action like a collision avoidance maneuver. Conjunction screening, the process of searching for potential conjunctions days in advance to avoid satellite collisions [27], has familiar requirements for capturing realistic satellite dynamics while retaining low computational cost. Realistic dynamics are important because the screening step is meant to identify candidate conjunctions for detailed inspection and follow-up. Low computational cost is important because the screening needs to be done regularly (several times per day) on the entire tracked catalog of objects. A key insight to be learned from the conjunction screening process is that collision risk is not uniform in time or space. For any pair of tracked objects there is at maximum two potential conjunction nodes where a close approach occurs. A collision between any two objects of interest is impossible if the objects are not near the conjunction nodes. Fig. 2 shows three potential orbital geometries that would result in zero, one, or two conjunction nodes for two orbits corresponding to a pair of tracked objects.

In conjunction screening, this concept of conjunction nodes helps to reduce the number of events that require computationally expensive high-fidelity orbital propagation analysis. The first pass check on potential conjunctions can be done with an assumption of Keplerian dynamics using the last issued TLEs for each object of interest. Once the conjunction nodes are identified, each can be analyzed based on the proximity of the conjunction and the orbit phasing of the satellites. In reality, conjunction geometries change over time as orbits are perturbed by non-Keplerian forces like Earth's higher order gravity terms, luni-solar interactions, atmospheric drag, and solar radiation pressure. The Keplerian dynamics used in this work allow for fast, analytical approximations of orbit geometries for short-term conjunction screening, and thus capture an instantaneous sustainability assessment for the populations under study.

3.2. Constraining conjunction frequency

The general procedure for identifying and constraining conjunction frequency across tracked objects is defined in Algorithm 1. For each pair of objects, we first identify their respective perigee and apogee radii according to

$$r_p = a(1-e) \tag{1}$$

$$r_a = a(1+e) \tag{2}$$

where a is the semi-major axis of the orbit and e is the eccentricity. A conjunction between a pair of objects may only occur if their altitude ranges overlap somewhere, or when

$$\max(r_{1p}, r_{2p}) \le \min(r_{1a}, r_{2a}), \tag{3}$$

where r_{1p} is the perigee radius for object 1 and r_{2a} is the apogee radius for object 2. If that condition is met, then we begin the procedure for identifying potential conjunctions. Computing the conjunction nodes for any two objects subject to Keplerian dynamics is straightforward from the basic equations of motion. The normal vector to the orbital plane is initially computed using each satellite's inclination (i) and right ascension of the ascending node (Ω).

Algorithm 1 Operationally Feasible Capacity Framework

Input: Catalog of objects with orbital elements from their latest TLEs.
for each unique pair of objects $(1, 2)$ in the TLE catalog **do**
  if $\max(r_{1p}, r_{2p}) \le \min(r_{1a}, r_{2a})$ **then**
    Identify the line of intersection of their orbital planes (or identify if they are coplanar).
    if orbital distances on the line of intersection are within 200 m **then**
      Compute the common period T_c, the time between conjunctions (should they occur).
      if $\neg\left(\left(T_c < 0.2\,\text{days}\right) \wedge \left(\text{name}_1 = \text{name}_2\right)\right)$ **then**
        Check whether a conjunction occurs within T_c given the initial orbit phasing.
        if a conjunction occurs within T_c **then**
          Record the conjunction node and nodal conjunction frequency $f_c^n = \left(T_c\right)^{-1}$.
        end if
      end if
    end if
  end if
end for
for each satellite in the catalog **do**
  Sum the satellite's nodal conjunction frequencies f_c^n to compute the satellite conjunction frequency f_c^s.
end for

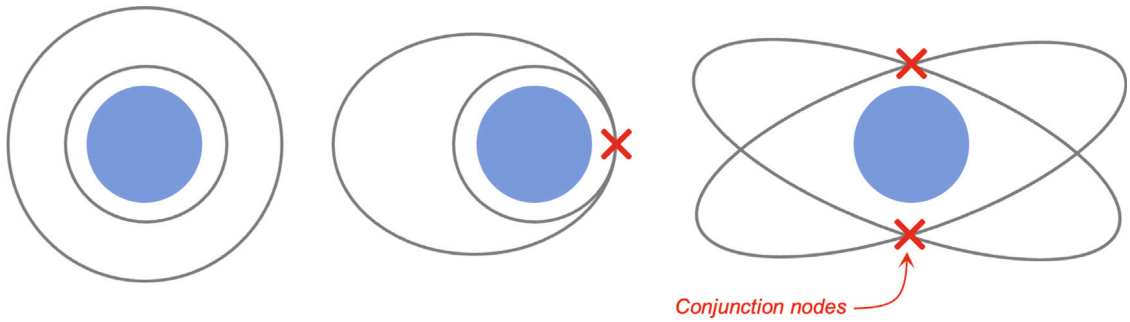

Fig. 2. Examples of orbital geometries resulting in zero, one, or two conjunction nodes.

For a pair of objects, the vector **n** normal to each object's orbit plane, is found by:

$$\mathbf{n}_1 = \begin{bmatrix} \sin(\Omega_1)\sin(i_1) \\ -\cos(\Omega_1)\sin(i_1) \\ \cos(i_1) \end{bmatrix}, \quad \mathbf{n}_2 = \begin{bmatrix} \sin(\Omega_2)\sin(i_2) \\ -\cos(\Omega_2)\sin(i_2) \\ \cos(i_2) \end{bmatrix}. \tag{4}$$

Given these normal vectors of two orbital planes, $\mathbf{n}_1$ and $\mathbf{n}_2$, the unit vector $\hat{\mathbf{m}}$ of the line of intersection between the planes is found by:

$$\hat{\mathbf{m}} = \frac{\mathbf{n}_1 \times \mathbf{n}_2}{\|\mathbf{n}_1 \times \mathbf{n}_2\|} \tag{5}$$

where $\times$ denotes the cross product and $\|\cdot\|$ is the L_2 norm. The next step is to compute the respective orbital radii along $\hat{\mathbf{m}}$. The radius r of a satellite from the focus is found by

$$r = \frac{a(1-e^2)}{1+e\cos(\nu)} \tag{6}$$

where ν is the true anomaly of the orbit. The apse line or direction of periapsis, $\hat{\mathbf{p}}$, is defined for each object as

$$\hat{\mathbf{p}}_1 = \frac{\mathbf{e}_1}{\|\mathbf{e}_1\|}, \quad \hat{\mathbf{p}}_2 = \frac{\mathbf{e}_2}{\|\mathbf{e}_2\|} \tag{7}$$

where $\mathbf{e}_1$ and $\mathbf{e}_2$ are the eccentricity vectors for orbits 1 and 2, respectively. The angle ϕ between the intersection line $\hat{\mathbf{m}}$ and each orbit's apse line is calculated as

$$\phi_1 = \arccos\left(\hat{\mathbf{m}} \cdot \hat{\mathbf{p}}_1\right), \quad \phi_2 = \arccos\left(\hat{\mathbf{m}} \cdot \hat{\mathbf{p}}_2\right). \tag{8}$$

For each direction along $\hat{\mathbf{m}}$, we compute the distance from the focus substituting ϕ for ν in Eq. (6). Thus, the position vectors of the closest approach points between the orbits are then

$$\begin{aligned} \mathbf{r}_1^A &= r^A(\phi_1)\cdot\hat{\mathbf{m}} \\ \mathbf{r}_2^A &= r^A(\phi_2)\cdot\hat{\mathbf{m}} \\ \mathbf{r}_1^B &= r^B(-\phi_1)\cdot -\hat{\mathbf{m}} \\ \mathbf{r}_2^B &= r^B(-\phi_2)\cdot -\hat{\mathbf{m}}. \end{aligned} \tag{9}$$

A conjunction node is identified when $\sqrt{\left(\mathbf{r}_1^A - \mathbf{r}_2^A\right)^2} < \epsilon$ or $\sqrt{\left(\mathbf{r}_1^B - \mathbf{r}_2^B\right)^2} < \epsilon$. The 18th and 19th space defense squadrons of the U.S. Space Force use default LEO screening volumes that are 400 m in the radial dimension. That means a potential conjunction is identified if the offset between two objects is less than 200 m, so $\epsilon = 200$ m in this work for consistency with that convention [28].

The procedure above is repeated for every pair of tracked satellites that passes through the apogee/perigee filter. For each pair, the positions of the closest orbital approach points are computed and stored. A conjunction node is only identified if the offset distance between the orbits is within ϵ. Note that the minimum distance at the conjunction nodes is technically distinct from the minimum orbital intersection distance (MOID), as we restrict our attention to offsets along the line of intersection between the orbital planes. While the true MOID need not lie on this line, any near-zero MOID—indicating a possible conjunction—must occur near it, since conjunctions are only possible where the two orbital planes intersect.

Every conjunction node has a characteristic nodal conjunction frequency which determines the rate at which the two satellites conjoin at the node. This nodal conjunction frequency is equivalent to the least common multiple (LCM) of the orbit periods for the pair of satellites conjoining at the node. This *common period*, T_c, measures the time between conjunctions at a conjunction node. It should not be confused with the synodic period, which measures the amount of time it takes for two objects to return to a reference orbit phasing. The common period enforces a requirement that an integer number of orbit periods has passed for each object, while the synodic period does not. T_c is found by:

$$T_c = qT_1 = pT_2, \quad \text{where } p, q \in \mathbb{Z}. \tag{10}$$

T_1 and T_2 are the orbital periods for satellites 1 and 2, respectively. The closest rational approximation for p and q is found within a tolerance of 10^{-3}, which enforces that the orbit crossings are within $\sim$1 s. Relative velocities for conjunctions in LEO average 10 km/s, which means the combined along-track and cross-track deviation between two objects over the one second threshold should be approximately 10 km. This offset is consistent with the standard LEO screening volumes referenced in the US Space Force's spaceflight safety handbook [28]. Fig. 3 shows that T_c is equivalent to the conjunction frequency at a conjunction node of interest. For a given primary object, secondary objects with orbit periods that are integer multiples of the primary's orbit period are in resonance. For example, two satellites that belong to a constellation may operate at the same orbit altitude but different planes, and thus would likely share two conjunction nodes. Those satellites will generally have close to a 1:1 resonance, meaning that if their orbits are properly maintained, their nodal crossings should be naturally de-conflicted. Instances when $T_c < 0.2$ days and the conjoining objects are both satellites that share a name (e.g. "STARLINK") are removed to screen out satellites that are in 1:1 resonance and are de-conflicted by design. For satellite pairs not de-conflicted by design, it is possible to experience *repeat conjunctions*, regular close approaches that cause a significant burden on conjunction assessment and collision avoidance systems. The conjunction frequency for each node, f_c^n, is equivalent to the inverse of the common period, $\left(T_c\right)^{-1}$.

In many cases, satellite pairs can go their entire common period without colliding. Since their orbital configuration resets after T_c, this is generally an indication that those objects should never collide according to the simplified Keplerian dynamics.

In order to identify whether a conjunction happens for every potential conjunction node, Kepler's equation is iteratively solved to compute the eccentric anomaly (E) for each satellite from the node. Kepler's equation is typically written

$$E = M + e\sin(M), \tag{11}$$

where M is the mean anomaly. E is solved iteratively by

$$E_{n+1} = E_n - \frac{E_n - e\sin E_n - M}{1 - e\cos E_n} \tag{12}$$

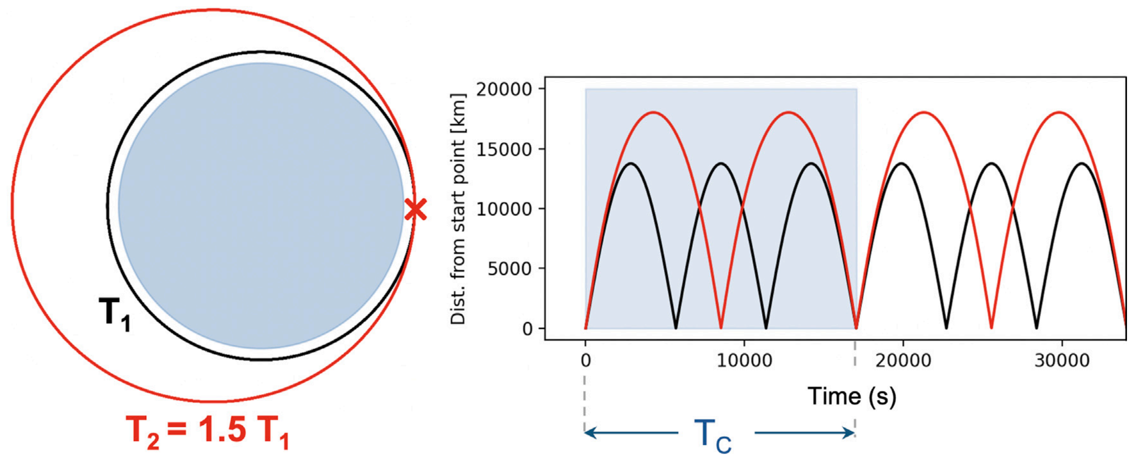

Fig. 3. T_c represents the period between conjunctions for any pair of objects. The figure depicts a simple example where $T_2 = 1.5\ T_1$.

until convergence. The angle ϕ between each orbit's apse line and the intersection line, calculated in Eq. (8), is used to find the eccentric anomaly of each conjunction point.

$$E = 2\arctan\left(\sqrt{\frac{1-e}{1+e}}\tan\frac{\phi}{2}\right) \tag{13}$$

Then, those eccentric anomaly values are used to calculate the transit time τ between each satellite's starting position at a reference time and arrival time at the conjunction point.

$$\tau = \frac{T}{2\pi}(E_c - E_0 - e(\sin E_c - \sin E_0)), \tag{14}$$

where T is the satellite's period, E_0 is the satellite's eccentric anomaly at the moment of assessment, and E_c is the eccentric anomaly of the conjunction point.

Given this transit time and a satellite's orbit, it is possible to generate a list of times when each satellite will arrive at the conjunction point. For example, if the transit time is $\tau = 500$ s, then the satellite will pass through the conjunction point 500 s after the start time. If that satellite has a period $T = 6000$ s, then it will return to the conjunction point at 6500 s, 12,500 s, 18,500 s, and so on. If a pair of satellites are both at the conjunction point at the same time (within some threshold Δt_{1-2}), then a conjunction has occurred.

One satellite may pass through many different conjunction nodes. Thus, it is necessary to sum the conjunction frequency across multiple nodes to compute a conjunction frequency for each satellite:

$$f_c^s = \sum_{i=1}^{n} f_c^n = \sum_{i=1}^{n} \left(T_{c_n}\right)^{-1} \tag{15}$$

Fig. 4 shows an example primary satellite and it's many conjoining secondary objects. The *satellite conjunction frequency* directly relates to the operational criticality, occupation, and capacity. f_c^s itself represents a criticality score, a method for ranking the existing population of satellites by their interactions with other objects. Capacity is a threshold on the criticality, above which operations become infeasible. While this threshold might vary among operators, this work considers a threshold of 10 conjunctions per month to be too frequent for feasible operations. For reference, the Starlink Gen 2 satellites performed 84,990 propulsive collision avoidance maneuvers between December 1, 2024 and May 1, 2025, which corresponds to 3.67 maneuvers per satellite per month [29]. In practice, these maneuvers are designed to reduce risk and are triggered when the probability of collision exceeds a set threshold at a defined lead time before the time of closest approach (TCA). For conjunctions with collision probability that falls below SpaceX's propulsive maneuver threshold, Starlink satellites may still perform "ducking" maneuvers (attitude changes that minimize the cross-sectional area in the conjunction plane), though public

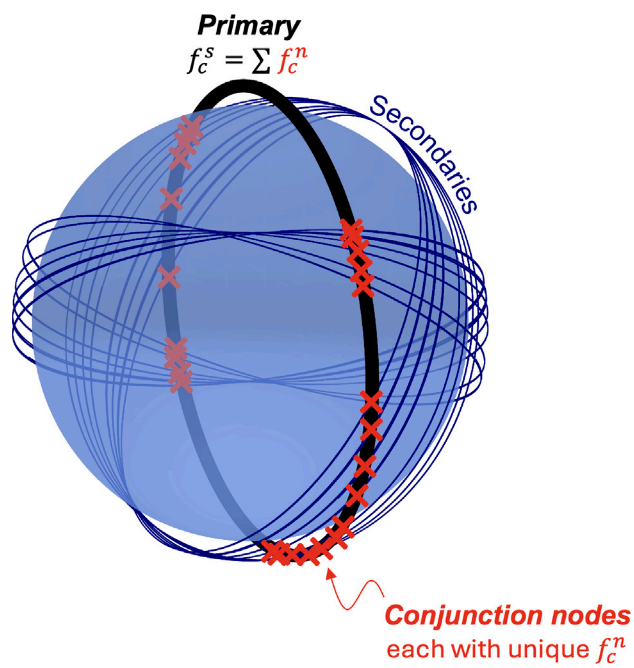

Fig. 4. Conjunction nodes for an example primary object. The primary's conjunction frequency is the sum of the nodal conjunction frequencies across all nodes.

data on the frequency of these events is unavailable. These ducking maneuvers certainly take place much more frequently than propulsive maneuvers because they are triggered by a lower collision probability threshold. While propulsive burns and ducking maneuvers are initiated using high-fidelity collision probability assessments rather than the purely geometric approach applied here with mean orbit elements, they nonetheless serve as a useful proxy for the frequency of risk-reduction actions and for understanding the practical limits of operator workload.

Occupation indicates how close each satellite is to exceeding the orbit's capacity. It is identified by the ratio of the satellite conjunction frequency f_c^s to the capacity threshold and indicates whether a particular orbit is feasible or not for operations. For example, if a satellite experiences 3 conjunctions per month, its criticality is 3 conjunctions per month and its occupation is 30% of the available capacity of 10 conjunctions per month. Similarly, we can identify particular nodes where the conjunction frequency approaches or exceeds our threshold.

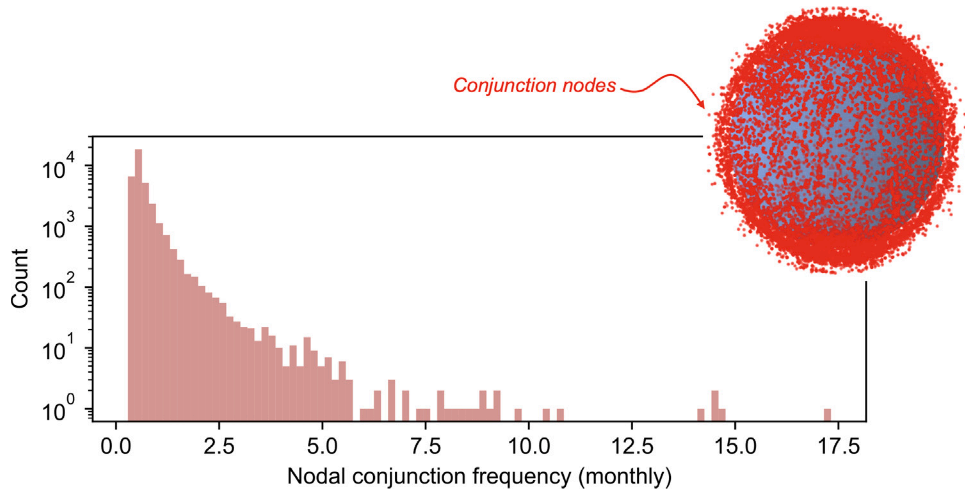

Fig. 5. Every conjunction node is assigned a nodal conjunction frequency, as determined by the inverse of T_c.

4. Results

4.1. Operational feasibility in the current LEO population (January 2025)

The operationally feasible capacity framework is tested using the orbital elements for the entire tracked catalog of objects in LEO, as taken from the U.S. Space Force Satellite Catalog (SATCAT) in January 2025, accessed via space-track.org. This population includes active satellites, derelict satellites, rocket bodies, and debris objects larger than 10 cm. Every possible pairing of objects is considered in the initial perigee-apogee screening. Orbital close approaches are identified for each pairing, and only close approaches with a node distance threshold of $\epsilon \leq 200$ meters are considered viable conjunction nodes. T_c is computed for every combination of satellites that results in a viable conjunction node. Instances when $T_c < 0.2$ days and the conjoining objects are both satellites that share a name are removed to screen out satellites that are in 1:1 resonance and are de-conflicted by design. As a final check for each node, a search over one common period is performed to retain all conjunction nodes in which the satellites pass through the node within 1 s of each other. If no conjunction occurs within the common period, a conjunction between those objects in the near future is unlikely. Fig. 5 shows the map of the remaining viable conjunction nodes based on this filtering process, along with the distribution of nodal conjunction frequencies across those nodes. A large majority of the conjunction nodes see $f_c^n < 2$ per month, but some clearly exceed our threshold of 10 conjunctions per month.

A high nodal conjunction frequency is achieved when an object pair has a low T_c and their orbit phases are not de-conflicted. Fig. 6 shows the distribution of conjunction nodes in altitude and latitude. A large portion of the viable conjunction nodes fall near 400–600 km, a busy region in LEO occupied by the Starlink constellation (~7000 satellites as of January 2025) among many other commercial operators, and near 700–800 km, a region that contains much of the debris from both the 2007 Fengyun-1C anti-satellite weapon test [30] and the 2009 Cosmos-Iridium satellite collision [31]. It should be noted that of all of the viable conjunction nodes identified in this work, 33.1% involve at least one Starlink satellite, while 68.3% involve at least one debris object. For reference, Starlink makes up 28.3% of the population and debris makes up 42.8%. Intra-constellation conjunctions are rare because constellations are passively de-conflicted. When actively managed, satellites are phased to avoid conjunctions entirely. This architecture does not, however, protect against conjunctions with other objects traversing the same region in orbital space. Starlink satellites are involved in a significant portion of the conjunction nodes because they represent a large and multitudinous target for all other objects in orbit.

Fig. 6 depicts a significant latitude dependence on conjunction node density. This distribution is explained by the fact that satellites spend more of their time in the extremities of their latitude bands which are dictated by the orbital inclination. Major spikes at around ±53° and ±82 ° make sense since large satellite populations sit around inclinations that should peak there (Starlink and sun-synchronous satellites, respectively).

Fig. 7 shows the cumulative density function (CDF) for the satellite conjunction frequency across the satellites under study in 2019, 2022, and 2025. The same analysis described previously for the 2025 case was also used for 2019 and 2022. The LEO catalog contained 13,741 objects in 2019, 20,704 objects in 2022, and 24,185 objects in 2025. Many of these satellites see a low conjunction frequency and thus would not require regular maneuvers or mitigation actions. In 2019, about 0.2% (or 27) of the tracked objects exceeded the 10 conjunction per month threshold, but by 2025 it was 1.4% (or 339 objects).

Fig. 8 depicts the total number of conjunction nodes compared to the population of tracked objects over time. The number of tracked objects and the number of conjunction nodes are very closely linked. Without enhanced coordination, the growing number of tracked objects will soon lead to even more conjunction nodes, a greater maneuver burden for operators, and an increased risk of collision.

4.2. Accounting for time-varying orbit geometries

The operational feasibility assessment procedure detailed thus far is an instantaneous representation of short-term sustainability, since it relies on a snapshot of orbital geometries from the TLE catalog. In reality, an object's orbit parameters change slowly over time from perturbations like Earth's higher-order gravity effects, variable atmospheric drag, solar radiation pressure, and luni-solar interactions. When we take that long-term variability into account, the conjunction node properties (count, distribution, frequency, etc.) change as well. In practice, this short-term analysis procedure may be repeated regularly to identify changes in the population properties over time. To highlight how dynamic orbit geometry impacts operational feasibility, we will focus on one long-term interaction between two example objects.

On February 28, 2024, an especially close approach between NASA's active TIMED satellite and Russia's defunct Cosmos 2221 satellite worried operators. At the time of closest approach, the offset distance between the satellites was less than 10 m, the relative velocity was approximately 14 km/s, and the probability of collision was 3%–8% [32, 33]. Neither spacecraft was capable of performing a collision avoidance maneuver.

Fig. 9 shows the offset distance at each of the conjunction nodes for TIMED and Cosmos 2221 throughout 2024. TLEs for each object

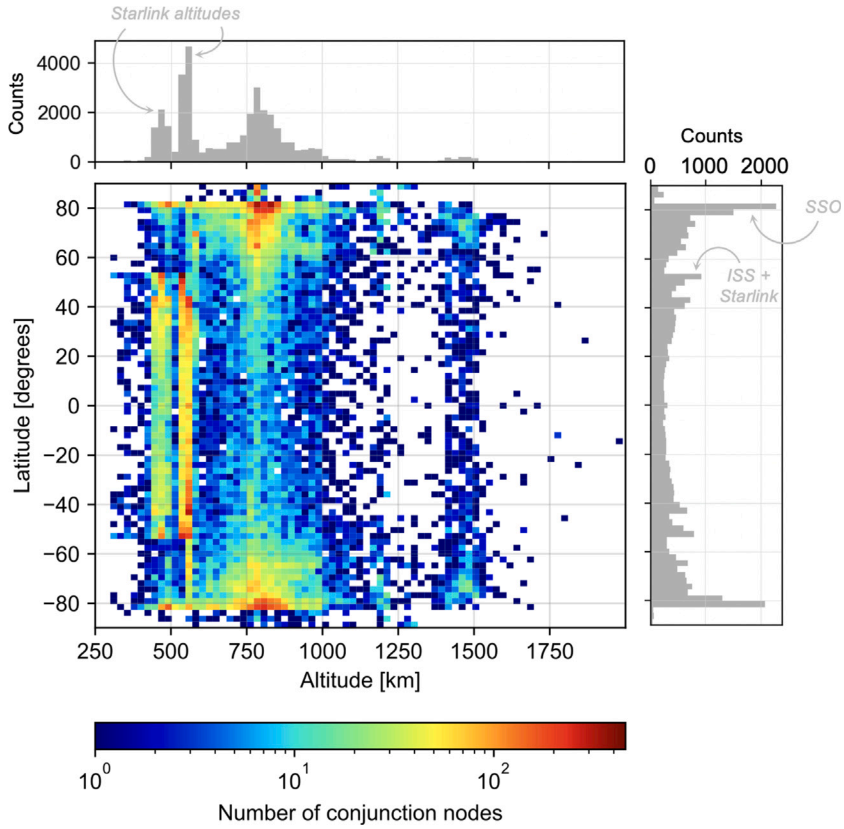

Fig. 6. Conjunction node position distributions across altitude and latitude for a snapshot in January 2025.

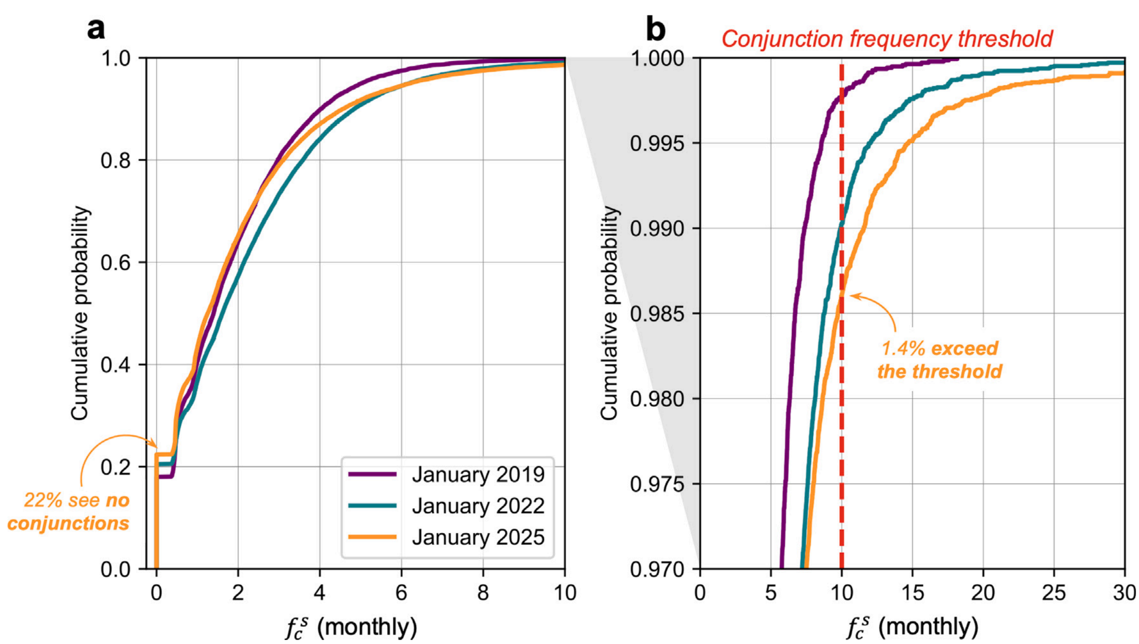

Fig. 7. Cumulative density function for satellite conjunction frequency from January 2019, 2022, and 2025. (a) shows the full CDF with a cutoff on the conjunction frequency, while (b) shows the top 3% of satellites by conjunction rate. Tracked object counts were 13,471, 20,704, and 24,185 in 2019, 2022, and 2025, respectively.

are updated multiple times per day and the varying orbit parameters are used to update their relative orbit geometry. Clearly, a conjunction between these two objects is not always possible. On the day of the very close approach, the offset distance at the conjunction nodes was very small and the orbit phasing between these two objects was unlucky, leading to the near-collision. The figure shows that in April 2024, for example, the probability of a collision between these objects was zero, since their minimum offset distance at the conjunction nodes was 5

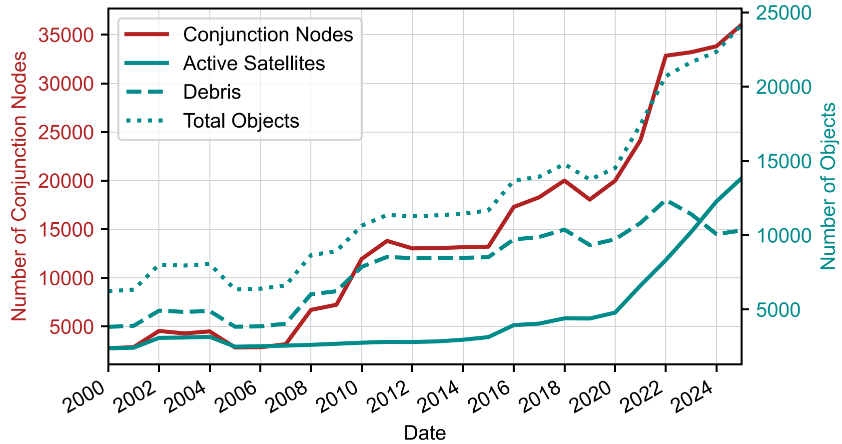

Fig. 8. Number of conjunction nodes and population of tracked objects from 2000 to 2025.

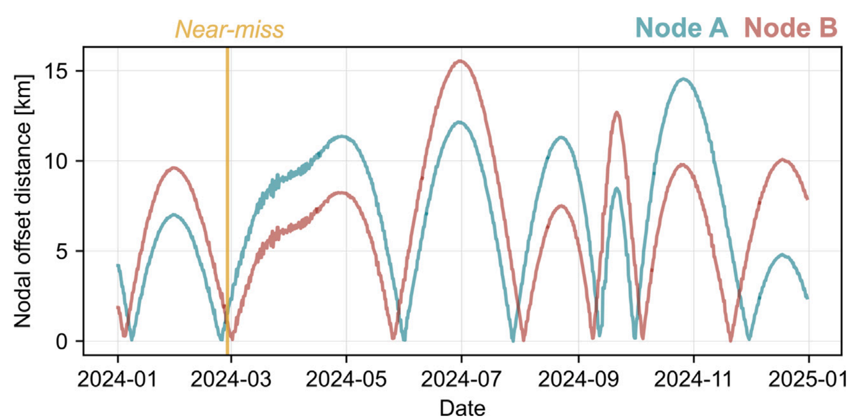

Fig. 9. Offset distances at nodes A and B for TIMED and Cosmos 2221 in 2024.

km. As orbital perturbations cause the relative geometry to shift over time, however, subsequent conjunction opportunities arise throughout the year.

5. Discussion and conclusion

This work developed an operational feasibility framework that maps a clear operator-centric constraint (conjunction frequency) to population-level assessments of orbital capacity, criticality, and occupation. Because there are infinitely many combinations of orbit geometries, the number of satellites that can operate within the operational feasibility threshold varies considerably depending on orbital structure.

In this analysis, the maximum acceptable conjunction rate per satellite was set at 10 conjunctions per month, beyond which the maneuver burden or collision risk becomes too high to justify continued operations. A differently assigned threshold will result in different (but similar) analysis outcomes. This is a top-down, environment-wide capacity threshold that is measured at the individual satellite level. The use of Keplerian dynamics enabled analytical computation of conjunction node geometry and frequency, though it simplifies the true orbital evolution. Over longer timescales, Earth's complex gravity field and atmospheric drag, among other forces, will perturb satellite motion; incorporating these higher fidelity effects for population-level assessments will be the subject of future work, though the conceptual framework presented here remains applicable.

Results show that the vast majority (98.6%) of LEO orbits do not exceed the 10 conjunctions per month threshold applied in this work. However, 339 objects were identified as exceeding this limit, primarily clustered between 400–600 km and 700–800 km altitudes. The satellite conjunction frequency thus serves as a criticality metric, highlighting satellites that impose frequent maneuver burdens or pose elevated collision risks relative to other satellites. The ratio between the criticality and the capacity threshold also informs the occupation metric, indicating how close each object is to exceeding capacity in its orbit.

Orbital structure plays a major role in determining sustainable satellite densities. Constellations typically manage intra-constellation conjunctions through careful de-conflicted orbit design but remain exposed to conjunctions with external objects. Indeed, a large portion of conjunction nodes identified in this work involve at least one large constellation satellite, such as those from Starlink, OneWeb, or Iridium.

Historically, large operators have assumed maneuver responsibility for most conjunctions with external objects, reducing maneuver burdens on others. However, this dynamic may not persist indefinitely given the lack of regulatory oversight in collision avoidance practices. Even with operator commitments, conjunction assessment remains imperfect, particularly during solar maximum and geomagnetic storms, and collision avoidance cannot eliminate risk entirely.

Removing tracked objects that see high conjunction rates could efficiently reduce aggregate collision risk, but it is also important to consider the origins of that risk. If a large constellation operator occupies an already populated region and argues that pre-existing satellites should be removed to facilitate its operations, this effectively displaces other users, asserting de facto eminent domain. In the absence of broad international agreements on space traffic management, operators are incentivized to launch rapidly and occupy orbital regions before others can, exacerbating congestion. Establishing clear space traffic management rules and access rights is critical to preventing a tragedy of the commons in orbit.

The actions of any single operator can significantly affect the operational feasibility of other spacecraft in nearby orbits. Without effective coordination, the rapid commercialization and expansion of space activities risks undermining the long-term sustainability of space operations. To ensure that near-Earth space remains operationally useful for generations to come, we must continue to develop mechanisms to measure, allocate, and coordinate access to orbital environments for the benefit of all.

Code availability

The code developed in this work is provided in https://github.com/ARCLab-MIT/operational_capacity.

CRediT authorship contribution statement

William E. Parker: Writing – review & editing, Writing – original draft, Visualization, Validation, Software, Resources, Project administration, Methodology, Investigation, Formal analysis, Data curation, Conceptualization. **Maya Harris:** Writing – review & editing, Writing – original draft, Visualization, Validation, Software, Methodology, Investigation, Formal analysis, Data curation, Conceptualization. **Giovanni Lavezzi:** Writing – review & editing, Writing – original draft, Supervision, Project administration, Methodology, Investigation, Formal analysis, Conceptualization. **Richard Linares:** Supervision, Project administration, Funding acquisition.

Declaration of generative AI and AI-assisted technologies in the manuscript preparation process

During the preparation of this work the authors lightly used ChatGPT in order to check and improve grammar. After using this tool, the authors reviewed and edited the content as needed and take full responsibility for the content of the published article.

Declaration of competing interest

The authors declare that they have no known competing financial interests or personal relationships that could have appeared to influence the work reported in this paper.

Acknowledgments

This research was sponsored by the Department of the Air Force Artificial Intelligence Accelerator and was accomplished under Cooperative Agreement Number FA8750-19-2-1000. The views and conclusions contained in this document are those of the authors and should not be interpreted as representing the official policies, either expressed or implied, of the Department of the Air Force or the U.S. Government. The U.S. Government is authorized to reproduce and distribute reprints for Government purposes notwithstanding any copyright notation herein.

Data availability

Two-line element datasets for tracked objects in the U.S. Space Force satellite catalog are available from https://celestrak.org and https://space-track.org.

References

[1] P. Del Monte-Luna, B.W. Brook, M.J. Zetina-Rejón, V.H. Cruz-Escalona, The carrying capacity of ecosystems, Glob. Ecol. Biogeogr. 13 (6) (2004) 485–495.

[2] F. Letizia, B.B. Virgili, S. Lemmens, Assessment of orbital capacity thresholds through long-term simulations of the debris environment, Adv. Space Res. 72 (7) (2023) 2552–2569.

[3] M. Lifson, Low Earth Orbit Spacecraft Slotting: Towards an Implementable Proposal (Ph.D. thesis), Massachusetts Institute of Technology, 2024.

[4] D.J. Kessler, B.G. Cour-Palais, Collision frequency of artificial satellites: The creation of a debris belt, J. Geophys. Res.: Space Phys. 83 (A6) (1978) 2637–2646.

[5] F. Letizia, C. Colombo, A. Rossi, A. Muciaccia, L. Giudici, R. Harada, S. Kawamoto, L. Böttcher, V. Ruch, C. Taillan, et al., Mission-based and environment-based approaches for assessing the severity of a space debris evolution scenario from a sustainability perspective, in: 75th International Astronautical Congress, IAC 2024, 2024, pp. 1–12.

[6] A. D'Ambrosio, S. Servadio, P.M. Siew, D. Jang, M. Lifson, R. Linares, Analysis of the LEO orbital capacity via probabilistic evolutionary model, in: 2022 AAS/AIAA Astrodynamics Specialist Conference, Vol. 11, Charlotte, North Carolina, August 7, 2022.

[7] A. Rossi, G.B. Valsecchi, E.M. Alessi, The criticality of spacecraft index, Adv. Space Res. 56 (3) (2015) 449–460, http://dx.doi.org/10.1016/j.asr.2015.02.027.

[8] F. Letizia, S. Lemmens, B.B. Virgili, H. Krag, Application of a debris index for global evaluation of mitigation strategies, Acta Astronaut. 161 (2019) 348–362.

[9] D. McKnight, E. Dale, M. Patel, C. Kunstadter, Modeling empirical orbital capacity, in: Space Capacity Allocation for the Sustainability of Space Activities Workshop, Politecnico Di Milan, 2023.

[10] A. D'Ambrosio, R. Linares, Carrying capacity of low earth orbit computed using source-sink models, J. Spacecr. Rockets (2024) 1–17, http://dx.doi.org/10.2514/1.A35729.

[11] D. Jang, Modeling the Future Space Debris Population and Orbital Capacity (Ph.D. thesis), Massachusetts Institute of Technology, 2024.

[12] W. Parker, M. Brown, R. Linares, Greenhouse gases reduce the satellite carrying capacity of low Earth orbit, Nat. Sustain. (2025).

[13] G. Lavezzi, D. Jang, R. Linares, Stable and sustainable orbital capacity solutions in Low Earth Orbit, Acta Astronaut. 235 (2025) 736–746, http://dx.doi.org/10.1016/j.actaastro.2025.06.015, URL https://www.sciencedirect.com/science/article/pii/S0094576525003662.

[14] C.C. Helms, A survey of launch services 2016–2020, in: AIAA Propulsion and Energy 2020 Forum, 2020, p. 3532.

[15] M.A. Rothblatt, Satellite communication and spectrum allocation, Am. J. Int. Law 76 (1) (1982) 56–77.

[16] M.J. Holzinger, M.K. Jah, Challenges and potential in space domain awareness, J. Guid. Control Dyn. 41 (1) (2018) 15–18.

[17] S. Eggl, Z. Benkhaldoun, G. Micheva, S.T. Spencer, D.V. Stark, B. Winkel, M. Rawls, M.W. Peel, SatHub panel: Satellite interference in observatories around the world, 2024, arXiv preprint arXiv:2408.15222.

[18] W. Ailor, R. Patera, Spacecraft re-entry strategies: meeting debris mitigation and ground safety requirements, Proc. Inst. Mech. Eng. Part G: J. Aerosp. Eng. 221 (6) (2007) 947–953.

[19] J. Dallas, S. Raval, J.A. Gaitan, S. Saydam, A. Dempster, The environmental impact of emissions from space launches: A comprehensive review, J. Clean. Prod. 255 (2020) 120209.

[20] J.P. Ferreira, K. Nomura, J. Wang, Preliminary assessment of the environmental impact of space debris demise during atmospheric reentry, in: Advanced Maui Optical and Space Surveillance Technologies (AMOS) Conference, 2023.

[21] NASA, NASA space sustainability strategy, 2024, URL https://www.nasa.gov/wp-content/uploads/2024/04/nasa-space-sustainability-strategy-march-20-2024-tagged3.pdf?emrc=676978822fa0b. (Accessed 4 February 2025).

[22] J.-C. Liou, The 2019 US Government Orbital Debris Mitigation Standard Practices, Tech. Rep., NASA, 2020.

[23] Inter-Agency Space Debris Coordination Committee (IADC), IADC Space Debris Mitigation Guidelines, Revision 1, Technical Report IADC-02-01, United Nations Office for Outer Space Affairs, Vienna, Austria, 2002, Revision 1 (September 2007) available at UNOOSA, URL https://www.unoosa.org/documents/pdf/spacelaw/sd/IADC-2002-01-IADC-Space_Debris-Guidelines-Revision1.pdf.

[24] A. Muciaccia, C. Colombo, D. McKnight, E. Dale, A. Rossi, Space capacity methodologies to rank the risk of orbital regions, in: Proceedings of the 9th European Conference on Space Debris, SDC-9, European Space Agency, Darmstadt, Germany, 2025, URL https://conference.sdo.esoc.esa.int/proceedings/sdc9/paper/223/SDC9-paper223.pdf.

[25] F. Letizia, S. Lemmens, B. Bastida Virgili, H. Krag, Application of a debris index for global evaluation of mitigation strategies, Acta Astronaut. 161 (2019) 348–362, http://dx.doi.org/10.1016/j.actaastro.2019.05.003.

[26] S. Servadio, N. Simha, D. Gusmini, D. Jang, T. St. Francis, A. D'Ambrosio, G. Lavezzi, R. Linares, Risk index for the optimal ranking of active debris removal targets, J. Spacecr. Rockets 1–14, http://dx.doi.org/10.2514/1.A35752.

[27] S. Alfano, D. Finkleman, On selecting satellite conjunction filter parameters, Acta Astronaut. 99 (2014) 193–200.

[28] 18th & 19th Space Defense Squadron, Combined Force Space Component Command, Spaceflight Safety Handbook for Satellite Operators, Version 1.7, Vandenberg Space Force Base, California, USA, Vandenberg Space Force Base, CA, USA, 2023, Version 1.7, URL https://www.space-track.org/documents/SFS_Handbook_For_Operators_V1.7.pdf.

[29] Space Exploration Holdings, LLC, Starlink Gen 1 and Gen 2 Semi-Annual Constellation Status Reports: December 1, 2024–May 31, 2025, Filing to the federal communications commission, Space Exploration Technologies Corp., Washington, DC, 2025, Letter to Marlene H. Dortch, Secretary, FCC; signed by David Goldman, URL https://www.scribd.com/document/883045105/SpaceX-Gen1-Gen2-Semi-Annual-Report-7-1-25.

[30] N.L. Johnson, E. Stansbery, J.-C. Liou, M. Horstman, C. Stokely, D. Whitlock, The characteristics and consequences of the break-up of the Fengyun-1C spacecraft, Acta Astronaut. 63 (1–4) (2008) 128–135.

[31] T. Kelso, et al., Analysis of the Iridium 33-Cosmos 2251 collision, Adv. Astronaut. Sci. 135 (2) (2009) 1099–1112.

[32] M. Wall, NASA satellite's 'shocking' space junk near-miss was even closer than thought, 2024, Published on Space.com; based on NASA analysis at the 39th Space Symposium, https://www.space.com/nasa-timed-satellite-russian-space-junk-near-miss-february-2024.

[33] USA TODAY Staff, NASA timed spacecraft passes safely by Russian satellite in close-call orbit, 2024, https://www.usatoday.com/story/news/nation/2024/04/23/nasa-timed-spacecraft-russian-satellite-near-collision/73421948007/. (Accessed 1 July 2025).